Modern Physics Letters A Vol. 4, No. 14 (1989) 1315–1328

SHORT RANGE CORRELATIONS AND NUCLEON EMISSION IN PERIPHERAL RELATIVISTIC HEAVY ION COLLISIONS

C. A. BERTULANI, L. F. CANTO and R. DONANGELO
Instituto de Física, Universidade Federal do Rio de Janeiro, Cx. Postal 68.528, 21945 Rio de Janeiro, RJ, Brasil

and

J. O. RASMUSSEN
Nuclear Science Division, Lawrence Berkeley Laboratory, 1 Cyclotron Road, Berkeley, California 94720, USA

Received 1 April 1989

We investigate the effects of short range correlations on nucleon emission in peripheral relativistic heavy ion collisions, following an idea originally proposed by Feshbach and Zabek. Expressions for one- and two-nucleon emission cross sections are derived and calculations for typical heavy ion systems are performed. We show that momentum conservation in the phonon absorption process leads to pronounced ridges in the quadruple-differential cross section for two-nucleon emission. We suggest that the presence of such ridges in future exclusive experiments should be considered as a signature of correlated emission of a nucleon pair.

1. Introduction

The study of relativistic heavy ion collisions (RHIC) over a decade has produced a wealth of interesting information.[1] Although the major efforts have been concentrated in central collisions, where there was hope of finding signatures of the quark-gluon state, distant and peripheral collisions have aroused considerable interest. In such cases, the collision partners preserve their identities and coherent processes play an important role. The excitation of the Giant Resonances through both electromagnetic and strong nuclear interactions have been considered by several authors.[2] At such energies, the collision time is very short and the action of the short range nuclear forces should excite the grazing region of the colliding nuclei. This excitation could equilibrate, forming a compound nucleus, and/or give rise to pre-equilibrium emission or other fast dissipation processes.

Bayman *et al.*[3] have approached the problem of energy deposition in peripheral RHICs, adopting straight line trajectories and using an impulse approximation for the interaction. These authors treat the nuclear matter classically and assume

that the nuclear surfaces do not have time to deform in response to the short pulse of nuclear field. The excitation energy is then determined by the calculation of the momentum transfer. Feshbach and Zabek[4] have considered the same problem from a different angle. These authors called attention to the special role played by nucleon pairs and their short-range correlations in peripheral RHICs. In such collisions, the projectile carries a mean field proportional to its density, which appears Lorentz contracted by the relativistic factor γ in the laboratory frame. If the projectile approaches the target with velocity v, the uncertainty relation associated to the variation of the field on a scale Δz (in the projectile frame) leads to the energy and the momentum of the nuclear interaction pulse

$$E \sim \frac{\hbar}{\Delta t} = \frac{\hbar v \gamma}{\Delta z} \quad p_z \sim \frac{\hbar \gamma}{\Delta z}. \tag{1.1}$$

For typical situations, Δz is a few Fermis and the nuclear interaction pulse can carry several hundred MeV. The cross section for nucleon emission induced by nuclear forces will depend on the probability that the target nucleons absorb this energy. Equation (1.1) shows that the field satisfies the dispersion relation $E = pv$ of a phonon. Feshbach and Zabek pointed out that the phonons could hardly be absorbed by a single nucleon since the latter would carry the momentum $\sim \sqrt{2mE}$, which is appreciably larger than that of Eq. (1.1). However, the phonon could be absorbed by a correlated nucleon-pair, which can have high kinetic energy and small total momentum, when the nucleons move along approximately opposite directions. These authors developed a semiclassical theory for the calculation of cross sections for this process.

The present work is concerned with the role of short range correlations in nucleon emission in peripheral RHICs. For this purpose, we use a model which is similar to that of Feshbach and Zabek.[4] Like these authors, we take straight line trajectories and use first order perturbation theory. However, we start with a nucleon-nucleus potential and adopt different wave functions for the bound nucleons. With the help of Gaussian approximations[5] for the potential and for the target nucleons, we obtain analytical expressions for the two-nucleon emission cross section and also take proper care of absorption effects. In Sec. 2, we introduce the theory and give the expressions for the cross sections. In Sec. 3, we apply the theory to nucleon emissions in the collisions Ca + Ca at 14.5 GeV/u and U + Ag at 1 GeV/u, discuss a possible signature of short range correlation effects. Finally, the main results of this work are summarized in Sec. 4.

2. Theoretical Treatment of the Short Range Correlation Effects

In this section, we study the effects of the short-range correlations in nucleon emissions induced by a peripheral relativistic heavy ion collision. We consider the coherent action of the projectile nucleons on each of the target nucleons. For

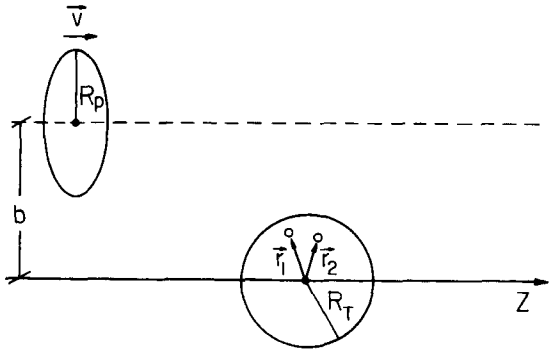

Fig. 1. The collision of a Lorentz contracted nucleus with a nucleon pair in a target nucleus.

this purpose, we represent this interaction by a Lorentz contracted nucleon-nucleus potential moving classically along the z-direction with constant velocity $v \approx c$, as illustrated in Fig. 1. To a first order perturbation approximation, the effect of such a potential is to alter the state of a single nucleon in the target. However, as shown by Feshbach and Zabek,[4] the state of a second nucleon correlated to the first one is also changed. To this order, the probability amplitude that the initial state of a nucleon pair in the target Ψ_i changes into a final state Ψ_f in a collision with impact parameter b is

$$a_{fi}(b) = \frac{1}{i\hbar}\int_{-\infty}^{\infty} dt\, e^{iwt} \int d^3r_1 d^3r_2\, \Psi_f^*(\mathbf{r}_1, \mathbf{r}_2)\,[V(\mathbf{r}_1, t) + V(\mathbf{r}_2, t)]\,\Psi_i(\mathbf{r}_1, \mathbf{r}_2) \qquad (2.1)$$

where $\hbar\omega = E_f - E_i$. Since we are interested in the emission of a pair of nucleons, we take for the final state the wavefunction

$$\Psi_f(\mathbf{r}_1, \mathbf{r}_2) = e^{i\mathbf{k}_1\cdot\mathbf{r}_1}\, e^{i\mathbf{k}_2\cdot\mathbf{r}_2} \qquad (2.2)$$

where $\mathbf{k}_i\,(i = 1,2)$, are the wave vectors of the emitted nucleons. In order to simplify the calculation of the integral appearing in Eq. (2.1), we consider Gaussian approximations for the potential $V(\mathbf{r}_i, t)$ and the nucleon orbitals in the initial state. The potential created by the projectile centered at the position (X,Y,Z), with $b = \sqrt{X^2 + Y^2}$ and $Z = vt$, is given by

$$V(\mathbf{r}_i, t) = \gamma\, V_g \exp\left\{-\frac{(X - x_i)^2}{\alpha_P^2}\right\} \exp\left\{-\frac{(Y - y_i)^2}{\alpha_P^2}\right\} \exp\left\{-\frac{\gamma^2\,(vt - z_i)^2}{\alpha_P^2}\right\}, \qquad (2.3)$$

where $\gamma = (1 - v^2/c^2)^{-1/2}$ is the standard relativistic factor introduced here to take into account the Lorentz contraction of the nucleonic density of the

projectile, which generates the potential. The strength V_g and the range parameter α_P are chosen so as to reproduce the magnitude and diffuseness of a Woods-Saxon potential at the nuclear surface. According to Karol's soft spheres approach,[5] these values are ralated to the Woods-Saxon radial and diffuseness parameters, R_P and a, respectively, by

$$V_g = \frac{V_0}{2} \exp\left\{\frac{R_P}{2a}\right\} \tag{2.4a}$$

and

$$\alpha_P = 2\sqrt{aR_P}. \tag{2.4b}$$

The initial wave function is given by

$$\Psi_i(\mathbf{r}_1, \mathbf{r}_2) = N_i \exp\left\{-\frac{r_1^2}{2\alpha_T^2}\right\} \exp\left\{-\frac{r_2^2}{2\alpha_T^2}\right\} \left[1 - \exp\left\{-\frac{|\mathbf{r}_1 - \mathbf{r}_2|^2}{r_c^2}\right\}\right], \tag{2.5}$$

where N_i is the appropriate normalization constant, r_c the correlation range and α_T the Gaussian width, related to the radius and diffuseness of the target density in a way similar to Eq. (2.4b).

The cross section for a transition $i \to f$ is given by the integral over impact parameter

$$\sigma_{fi}(\mathbf{k}_1, \mathbf{k}_2) = 2\pi \int_{R_T+R_P}^{\infty} |a_{fi}(b)|^2 \, b \, db. \tag{2.6}$$

We have set the impact parameter cutoff at $b = R_P + R_T$ in order to account for the strong absorption effects that arise in close collisions. Substituting Eqs. (2.1–5) into Eq. (2.6) and performing the integrations (see the Appendix for details), we obtain

$$\sigma_{fi}(\mathbf{k}_1, \mathbf{k}_2) = K \exp\left\{-\frac{aR_P\omega^2}{\gamma^2 c^2}\right\} \left[\exp\left\{-\frac{k_1^2 r_c^2}{4}\right\} + \exp\left\{-\frac{k_2^2 r_c^2}{4}\right\}\right]^2$$
$$\times \exp\left\{-2aR_T\left(k_{1z} + k_{2z} - \frac{\omega}{c}\right)^2\right\} \exp\left\{-\frac{aR_T}{\mathcal{A}}|\mathbf{k}_{1T} + \mathbf{k}_{2T}|^2\right\}, \tag{2.7}$$

where $\mathcal{A}$ is the factor $(1/2)\,(1 + R_T/R_P)$, K is the multiplicative constant of Eq. (A.10), and k_{iz}, $\mathbf{k}_{iT}$ $(i = 1, 2)$ are the axial and transverse components of $\mathbf{k}_i$ $(i = 1, 2)$, respectively.

The cross section for emission of a correlated nucleon pair can be obtained by

multiplication of Eq. (2.7) by the density of final plane wave states, $d^3k_1\, d^3k_2/(2\pi)^6$, and by the number of nucleon pairs in the target $A_T(A_T - 1)/2 \simeq A_T^2/2$. In terms of the kinetic energies $\varepsilon_1, \varepsilon_2$ and the directions (θ_1, ϕ_1), (θ_2, ϕ_2) of the two nucleons, this cross section is

$$\frac{d^4\sigma}{d\varepsilon_1 d\varepsilon_2 d\Omega_1 d\Omega_2} = K' \sqrt{\varepsilon_1 \varepsilon_2}\, P(\varepsilon_1, \varepsilon_2)\, M_z(\varepsilon_1\theta_1, \varepsilon_2\theta_2)\, M_T(\varepsilon_1\theta_1\phi_1, \varepsilon_2\theta_2\phi_2). \tag{2.8}$$

In Eq. (2.8), K' is the constant

$$K' = \frac{9}{32} A_T^2 \frac{r_c^6\, a^5\, R_P^2}{\mathcal{A} R_T^3} \frac{V_0^2\,(mc^2)^3}{(\hbar c)^8} \left(\frac{c}{v}\right)^2 \exp\left\{-\frac{R_T - R_P}{2a}\right\}, \tag{2.9}$$

where m is the nucleon and A_T is the target mass number. P is the phonon spectrum factor, given by

$$P = \exp\left\{-\left(\frac{\varepsilon_1 + \varepsilon_2 + B}{\Delta_P}\right)^2\right\}. \tag{2.10}$$

C is the correlation factor given by

$$C = \left[\exp\left\{-\frac{\varepsilon_1}{\Delta_c}\right\} + \exp\left\{-\frac{\varepsilon_2}{\Delta_c}\right\}\right]^2 \tag{2.11}$$

and M_z and M_T are the momentum conservation factors

$$M_z = \exp\left\{-\frac{\left(\sqrt{\varepsilon_1}\cos\theta_1 + \sqrt{\varepsilon_2}\cos\theta_2 - (\varepsilon_1 + \varepsilon_2 + B)/\sqrt{2mc^2}\right)^2}{\Delta_M}\right\} \tag{2.12}$$

$$M_T = \exp\left\{-\frac{\varepsilon_1 \sin^2\theta_1 + \varepsilon_2 \sin^2\theta_2 + 2\sqrt{\varepsilon_1\varepsilon_2}\sin\theta_1 \sin\theta_2 \cos(\phi_1 - \phi_2)}{2\mathcal{A}\Delta_M}\right\}. \tag{2.13}$$

Above, B is the binding energy of the nucleon pair in the target and Δ_P, Δ_C and Δ_P are the energy widths.

$$\Delta_P = \frac{\gamma\hbar v}{\sqrt{2aR_P}} \tag{2.14a}$$

$$\Delta_C = \frac{2(\hbar c)^2}{mc^2 r_c^2} \tag{2.14b}$$

$$\Delta_M = \frac{(\hbar c)^2}{4mc^2\, a\, R_T}. \tag{2.14c}$$

The total cross section for the emission of a nucleon with energy ε along the direction specified by the angles (θ, ϕ) can be obtained by integration of Eq. (2.8), with the help of Eqs. (2.9–14). The integral over the azimuthal angle can be performed analytically and we get

$$\frac{d^2\sigma}{d\varepsilon d\Omega} = 2\pi K' \sqrt{\varepsilon} \int_0^\infty d\varepsilon' \sqrt{\varepsilon'} \int_0^\pi d\cos\theta'\, P(\varepsilon, \varepsilon')\, C(\varepsilon, \varepsilon')\, M_z(\varepsilon\theta, \varepsilon'\theta')$$

$$\times I_0\left(\frac{\sqrt{\varepsilon\varepsilon'}\sin\theta\sin\theta'}{\mathcal{A}\Delta_M}\right) \exp\left\{-\frac{\varepsilon\sin^2\theta + \varepsilon'\sin^2\theta'}{2\mathcal{A}\Delta_M}\right\}, \tag{2.15}$$

where I_0 is the modified Bessel function of zeroth order.

In the next section, we show several examples of application of the formulae for the one- and two-nucleon emission cross sections developed above.

3. One- and Two-Nucleon Emissions in High-Energy Peripheral Collisions

We now consider the application of the theory of Sec. 2 to reactions induced by high energy heavy ion beams. The first example is the ^{40}Ca + ^{40}Ca system at 14.5 GeV/u which can be studied with the Ca beam that will be soon available at Brookhaven. The other is the ^{238}U + ^{nat}Ag system at 1 GeV/u, experimentally studied (albeit for purposes different than those pursued in the present work) by Friedlander *et al.*[6] with the Berkeley Bevalac. In this case, we consider the nucleon pair emission from the uranium nucleus. Consequently, we work in the uranium-fixed frame of reference.

We first consider the quadruple-differential cross section of Eq. (2.8). The parameter values $r_0 = 1.2$ fm, $r_c = 0.7$ fm, $a = 0.65$ fm, and $B = 16$ MeV utilized lead to the energy widths for the two systems appearing in Table 1.

Several interesting conclusions can be drawn from inspection of the Table I and Eqs. (2.14). First of all, we notice that the energy width associated to the nucleon-nucleon correlation range, Δ_C, is independent of both the projectile-target combination and the projectile energy. A second remark is that the energy width Δ_P of the phonon spectrum depends strongly on the incident energy but

Table 1. The energy widths in the two-nucleon emission cross section.

System	Δ_P(MeV)	Δ_C(MeV)	Δ_M(MeV)
Ca+Ca	1420	171	3.9
U+Ag	134	171	2.2

weakly on the system size. From the relation between the Δ_P and Δ_C values, we expect that the correlation factor C will predominate over P in determining the behavior of the cross sections for the Ca + Ca system at 14.5 GeV/u, while both factors should be about equally important in the U + Ag case at 1 GeV/u. Finally, the small values of the Δ_M parameters in both cases suggest that the momentum conservation factors M_z and M_T strongly correlate the angles and energies at which the two nucleons are emitted. Inspection of Eq. (2.12) indicates, however, that the exponent of M_z does not have a linear dependence on ε_1 and ε_2. Therefore Δ_M does not give a direct measure of the energy spread of the cross section. We comment further on these factors later in this section.

In Fig. 2, we illustrate the calculated cross section for a forward-backward ($\theta_1 = 0°$, $\theta_2 = 180°$) nucleon pair emission for the two systems considered. The curves of equal quadruple-differential cross section plotted as a function of the final kinetic energies of the two nucleons were calculated using Eq. (2.8). As mentioned above, there is a strong correlation between the nucleon energies, resulting, in this case, from the M_z factor. The effect of this factor is to produce a

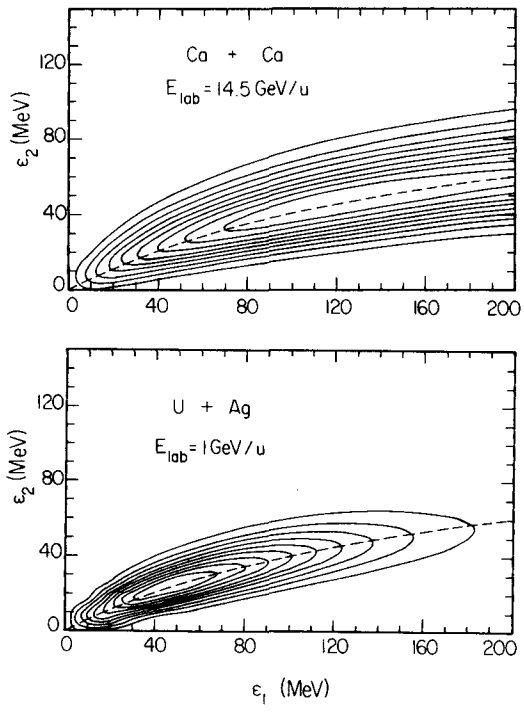

Fig. 2. The quadruple-differential cross section ($d^4\sigma/d\varepsilon_1 d\varepsilon_2 d\Omega_1 d\Omega_2$) of Eq. (2.8) for $\theta_1 = 0°$ and $\theta_2 = 180°$, as a function of ε_1 and ε_2. The cross sections are given in arbitrary units. The calculations were performed in the rest frames of one of the Ca nuclei and the U nucleus, respectively.

ridge in the cross section, which is determined by the values of ε_1 and ε_2 for which the exponent appearing in M_z vanishes. This condition defines the curve

$$\varepsilon_1 + \varepsilon_2 + B = \sqrt{2mc^2}\left(\sqrt{\varepsilon_1} - \sqrt{\varepsilon_2}\right), \tag{3.1}$$

represented in Fig. 2 by dashed lines, which describe the ridge to a good approximation. As the general form of Eq. (3.1) suggests, the location of the ridge is a kinematical property of the phonon absorption mechanism, which is independent of the system or the collision energy. It is interesting to notice that for emissions on the ridge the forward going nucleon carries a larger energy. This is a direct consequence of the fact that the absorbed phonon carries momentum along the beam direction. The other terms in Eq. (2.8) lead to slight changes in the shape of the ridge, and more importantly, give rise to the broad maximum observed at $\varepsilon_1 = 125$ MeV, $\varepsilon_2 = 47$ MeV, in the Ca + Ca case, and a sharper one at $\varepsilon_1 = 47$ MeV, $\varepsilon_2 = 24$ MeV, in the U + Ag case. The narrower ridge obtained in the latter arises from its smaller width Δ_M. Larger systems possess larger interaction regions, which causes a sharper definition of the energy transferred.

The factor M_T played no role in this first example since it is identically equal to one. In order to observe transverse momentum effects on the two-nucleon emission, we consider the situation where one of the nucleons is emitted at right angles to the beam, $\theta_1 = 90°$, and, for the sake of definiteness, we also fix its energy at $\varepsilon_1 = 50$ MeV, for which both systems have appreciable cross sections. In Fig. 3, we plot the same quadruple-differential cross section of Eq. (2.8) as a function of the nucleon 2 observables ε_2 and θ_2. For simplicity, we consider that both nucleons are emitted in a plane containing the beam direction, i.e., we set $\phi_1 - \phi_2 = 180°$. We immediately notice that the emission of nucleon 2 is strongly correlated in energy and angle with that of nucleon 1. In this case, the maximum cross section occurs for emission energies and directions such that the exponents of M_z and M_T are both approximately equal to zero. This means that the most probable emission is such that the transverse momentum of the nucleon pair vanishes and the longitudinal momentum of the pair is equal to that of the absorbed phonon, ω/c. This situation is depicted in the insets appearing in Fig. 3. From the contour lines in this figure, we note that the cross section for emission of a nucleon pair is quite concentrated around the angle corresponding to the maximum ($\theta_2 \approx 68°$ in both cases).

The properties of the quadruple-differential cross-sections illustrated in Figs. 2 and 3 are the signature of the nucleon pair emission via the short range nucleon-nucleon correlations. It could be interesting to evaluate the contribution of this process to the single nucleon spectra. As shown in Sec. 2, this can be obtained by partial integration of the cross section discussed above, leading to Eq. (2.15). As an example, we show the nucleon spectra that result from the U + Ag collision at

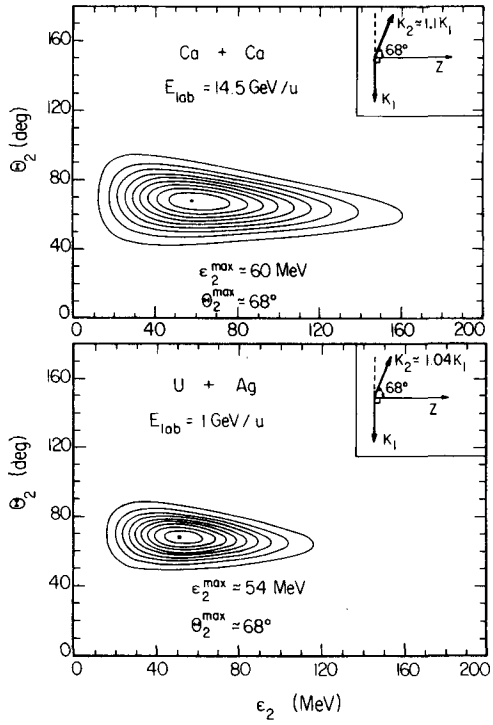

Fig. 3. The cross section of Fig. 2 as a function of θ_1 and ε_1. The energy and direction of the first nucleon are kept fixed at $\theta_1 = 90°$ and $\varepsilon_1 = 50$ MeV. The values of θ_2^{max} and ε_2^{max}, where the cross section is a maximum, are indicated. The inset shows the wave numbers $\mathbf{k}_1$ and $\mathbf{k}_2$ corresponding to this maximum. The rest frames are the same as in Fig. 2.

several observation angles (see Fig. 4). In contrast to the energy spectra that arise from a single nucleon knock-out, or the decay of a giant resonance excited in the collision, we notice that in this case the distribution reaches very high energies, especially in the case of forward angles.

In order to assess the relative importance of this mechanism of nucleon emission, we have estimated the total cross section by numerical integration of Eq. (2.15) over the nucleon emission angle and energy. Using a potential strength $V_0 = 50$ MeV, we find $\sigma \simeq 85$ mb in the Ca + Ca case and $\sigma \simeq 30$ mb for the U + Ag system, at the same collision energies used before. In spite of its relatively small value, when compared to the total reaction cross section, we think that it may be possible to extract a signature of this process. This could be done, for example, through the study of correlations in the two-nucleon production data.

It is important to realize that the cross section values we have calculated are considerably smaller than those obtained by Feshbach and Zabek for similar systems, which exceed one barn.[4] It is difficult to pinpoint the origin of this discrepancy since each work uses many different approximates. We would argue,

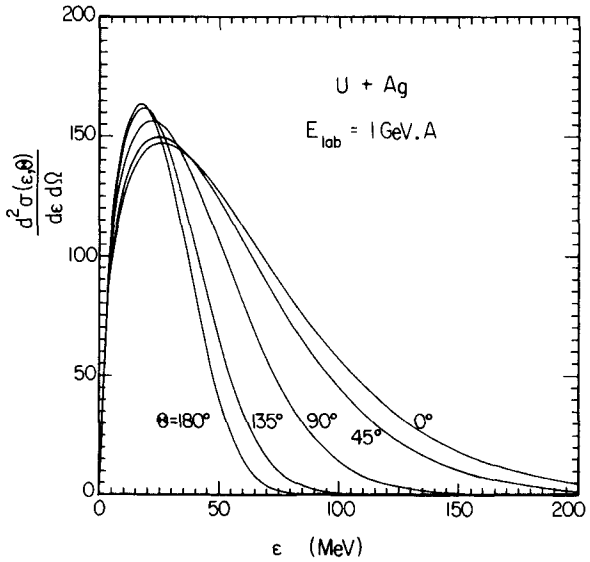

Fig. 4. The one-nucleon emission spectrum (Eq. (2.15)) at several observation angles in the U rest frame. The cross sections are given in arbitrary units.

however, that our results are more consistent with the peripheral nature of the process and with the first order perturbation treatment employed in both works. Being a peripheral process, its cross section may be written in the form $\sigma \sim 2\pi\Delta(R_P + R_T)\mathscr{P}$, where $\Delta \simeq 1$ fm is the impact parameter range for grazing collisions, and $\mathscr{P}$ the average probability for this reaction to occur within this interval. Since $2\pi\Delta(R_P + R_T) < 1$b, it appears that the results of Ref. 4 overestimate the cross section. Besides, the perturbation approximation requires $\mathscr{P} \ll 1$, so that while our results are consistent with this constraint, those of Ref. 4 would require $\mathscr{P} \approx 1$ in order to reach the high cross section values it finds.

4. Conclusions

We have studied the effect of the short range nucleon-nucleon correlations on the emission of one or two nucleons from a heavy target induced in a peripheral relativistic heavy ion collision. We have used Gaussian approximations for the nucleon-nucleus potential and for each nucleon-pair wave function. In this way, we took into account absorption effects explicitly and derived an analytical expression for the quadruple-differential cross section for the emission of two nucleons. This cross section is written as the product of several factors: a phonon spectrum, analogous to the one discussed by Feshbach and Zabek, a factor explicitly dependent on the correlation radius, and factors associated to momentum conservation in the absorption of a phonon by a correlated nucleon

pair. We have performed numerical calculations for the Ca + Ca and U + Ag systems at 14.5 GeV/u and 1 GeV/u, respectively. The calculated cross sections display a marked correlation between the energies and directions of the emitted nucleons. We have shown that these correlations predominantly arise from momentum exchange btween the nucleon pair and the absorbed phonon. It is suggested that such correlations can be used as a signature for short range correlation effects in future exclusive experiments, since our estimate for the total cross section for this mechanism lies in the few tens of millibarns range. We have not attempted to compare these predictions with experiment in this work since such exclusive experimental data does not appear to be available at present.

Acknowledgments

This work was supported in part by the Financiadora de Estudos e Pesquisas — Brazil, in part by the Director, Office of Energy Research, Division of Nuclear Physics of the Office of High Energy Research and Nuclear Physics of the U.S. Department of Energy under Contract DE-AC03-76SF00098, and in part by a cooperative research grant INT-8302853 of the National Science Foundation and the Conselho Nacional de Pesquisas e Desenvolvimento Científico.

We would like to acknowledge G. E. Brown and M. S. Hussein for stimulating discussions, and P. Carrilho for helping with the numerical calculations.

APPENDIX

In this appendix, we give details of the derivation of Eq. (2.7).

Substituting Ψ_i (Eq. (2.5)), Ψ_f (Eq. (2.2)) and V (Eq. (2.3)) in Eq. (2.1), and then taking the absolute value, we get

$$a_{fi}(b) = \frac{N_i \gamma V_g}{i\hbar} \sum_{j=1}^{2} \int d^3r_1 d^3r_2 \exp\left\{-\frac{r_1^2+r_2^2}{2\alpha_T^2} - \frac{|\mathbf{r}_1-\mathbf{r}_2|^2}{r_c^2}\right\} \times \exp\left\{-\frac{x_j^2 + (b-y_j)^2}{\alpha_P^2} - i(\mathbf{k}_1\cdot\mathbf{r}_1 + \mathbf{k}_2\cdot\mathbf{r}_2)\right\} \times \int_{-\infty}^{\infty} dt \exp\left\{-\gamma^2 \frac{(z_j - vt)^2}{\alpha_P^2} + i\omega t\right\}. \tag{A.1}$$

The integration over time can be easily performed,[7] we get the value

$$\frac{2\sqrt{\pi a R_P}}{\gamma v} \exp\left\{izj\frac{\omega}{v}\right\} \exp\left\{-\frac{aR_P\omega^2}{\gamma^2 v^2}\right\}, \tag{A.2}$$

and Eq. (A.1) gives

$$|a_{fi}(b)|^2 = \frac{4|N_i V_g|^2 \pi a R_P}{\hbar^2 v^2} \left| \sum_{j=1}^{2} I_j \right|^2 \exp\left\{ -\frac{a R_P \omega^2}{\gamma^2 v^2} \right\}. \tag{A.3}$$

In Eq. (A.3), I_j is the integral

$$I_j = \int d^2r_1\, d^3r_2 \exp\left\{ -\frac{r_1^2+r_2^2}{2\alpha_T^2} - \frac{|\mathbf{r}_1-\mathbf{r}_2|^2}{r_c^2} - \frac{x_j^2+(b-y_j)^2}{\alpha_P^2} \right\}$$
$$\times \exp\left\{ -i\left(\mathbf{k}_1\cdot\mathbf{r}_1 + \mathbf{k}_2\cdot\mathbf{r}_2 - \frac{\omega}{c} \right) z_j \right\}, \tag{A.4}$$

The integral I_j can be written as a product of the cartesian factors I_{jx}, J_{jy} and I_{jz}, given by

$$I_{jx} = \int_{-\infty}^{\infty} dx_1 \int_{-\infty}^{\infty} dx_2 \exp\left\{ -\frac{x_1^2 + x_2^2}{2\alpha_T^2} - \frac{(x_1 - x_2)^2}{r_c^2} - \frac{x_j^2}{\alpha_P} \right\}$$
$$\times \exp\{-i\,(k_{1x}x_1 + k_{2x}x_2)\}, \tag{A.5a}$$

$$I_{jy} = \int_{-\infty}^{\infty} dy_1 \int_{-\infty}^{\infty} dy_2 \exp\left\{ -\frac{y_1^2 + y_2^2}{2\alpha_T^2} - \frac{(y_1 - y_2)^2}{r_c^2} - \frac{(b - y_j)^2}{\alpha_P^2} \right\}$$
$$\times \exp\{-i\,(k_{1y}y_1 + k_{2y}y_2)\}, \tag{A.5b}$$

and

$$I_{jz} = \int_{-\infty}^{\infty} dz_1 \int_{-\infty}^{\infty} dz_2 \exp\left\{ -\frac{z_1^2 + z_2^2}{2\alpha_T^2} - \frac{(z_1 - z_2)^2}{r_c^2} \right\}$$
$$\times \exp\left\{ -i\left(k_{1z}z_1 + k_{2z}z_2 - \frac{\omega}{c} z_j \right) \right\}. \tag{A.5c}$$

The integrals above can be carried out analytically and we get

$$I_{1x} = \pi\mu\rho \exp\left\{ -\frac{\mu^2 k_{2x}^2}{4} \right\} \exp\left\{ -\frac{\rho^2}{4}(k_{1x} + \delta k_{2x})^2 \right\}, \tag{A.6a}$$

$$I_{1y} = \pi\mu\rho \exp\left\{ -\frac{\mu^2 k_{2y}^2}{4} \right\} \exp\left\{ -\frac{\rho^2}{4}\left[\frac{2b}{\alpha_P^2} + i(k_{1y} + \delta k_{2y}) \right]^2 \right\} \exp\left\{ -\frac{b^2}{\alpha_P^2} \right\}, \tag{A.6b}$$

and

$$I_{1z} = \pi\mu\rho \exp\left\{-\frac{\mu^2 k_{2z}^2}{4}\right\} \exp\left\{-\frac{\rho^2}{4}(k_{1z} + \delta k_{2z}) - \frac{\omega}{c})^2\right\}, \tag{A.6c}$$

and similar expressions for $j = 2$, interchanging the subindices 1 and 2. Above μ, ρ and δ stand for

$$\mu = \left(\frac{1}{2\alpha_T^2} + \frac{1}{r_c^2}\right)^{-1/2}, \tag{A.7a}$$

$$\rho = \left(\frac{1}{2\alpha_T^2} + \frac{1}{r_c^2} + \frac{1}{\alpha_P^2} - \frac{\mu^2}{r_c^4}\right)^{-1/2}, \tag{A.7b}$$

and

$$\delta = \frac{\mu^2}{r_c^2}. \tag{A.7c}$$

We are interested in the effects of short range correlations, which satisfy the condition $r_c^2 \ll \alpha_T^2, \alpha_P^2$. In this case, the parameters μ, ρ and δ can be evaluated to lowest order in r_c^2/α_T, and we get

$$\mu \approx r_c \quad \delta \approx 1 \quad \rho \approx \frac{\alpha_T}{\sqrt{2\mathcal{A}}} = \sqrt{\frac{2aR_T}{\mathcal{A}}}, \tag{A.8}$$

where $\mathcal{A}$ is the factor $1/2(1 + R_T/R_P)$, which reduces to unity when the projectile and the target have the same mass number. Substituting these results in Eq. (A.1) and evaluating the integral over impact parameters, we get

$$\sigma_{fi}(\mathbf{k}_1, \mathbf{k}_2) = K \exp\left\{-\frac{aR_P\omega^2}{\gamma^2 v^2}\right\}\left[\exp\left\{-\frac{k_1^2 r_c^2}{4}\right\} + \exp\left\{-\frac{k_2^2 r_c^2}{4}\right\}\right]^2$$
$$\times \exp\left\{-2aR_T\left(k_{1z} + k_{2z} - \frac{\omega}{c}\right)^2\right\} \exp\left\{-\frac{aR_r}{\mathcal{A}}|\mathbf{k}_{1T} + \mathbf{k}_{2T}|^2\right\} \tag{A.9}$$

where

$$K = \frac{9\, r_c^6\, a^5\, R_P^2 |V_0|^2}{16\, R_T^3 \gamma^2 \hbar^2 v^2 \mathcal{A}} \exp\left\{-\frac{R_T - R_P}{2a}\right\}. \tag{A.10}$$

As we have discussed in Sec. 3, the momentum conservation factors appearing in Eq. (A.9) (the last two exponentials) play a most important role in the two-nucleon emission cross section. They allow for the emission of very energetic

nucleons such that the nucleon pair has negligible transverse momentum ($\mathbf{k}_{1T} \simeq \mathbf{k}_{2T}$) and net longitudinal momentum $k_{1z} + k_{2z} \simeq w/c$. This is possible because the short range correlations ($\delta = 1$) couples the momenta of the two nucleons. If the correlations have long range, or the nucleons are not correlated, one should take the limit $r_c \to \infty$, which leads to $\delta \to 0$. In this case, the momenta of the two nucleons decouple and the emission of an energetic nucleon is strongly hindered by the momentum conservation factors.

References

1. See, e.g., *Proc. of the XI Int. Conf. on Particles and Nuclei*, Kyoto, 1987, eds. S. Homma, M. Morita, K. Nakai and T. Yamazaki, *Nucl. Phys.* **A478** (1978).
2. C. A. Bertulani and G. Baur, *Phys. Rep.* **163** (1988) 299; J. O. Rasmussen, J. S. Blair and X. J. Qiu, *Proc. Workshop on Nuclear Physics*, Philadelphia, 1980 (Plenum, 1982); J. O. Rasmussen, L. F. Canto and X. J. Qiu, *Phys. Rev.* **C33** (1986) 2033.
3. B. F. Bayman, P. J. Ellis, S. Fricke and I. C. Tang, *Phys. Rev Lett.* **53** (1984) 1322; **53** (1984) 2516; **49** (1982) 532.
4. H. Feshbach and M. Zabek, *Ann. of Phys.* **107** (1977) 110; H. Feshbach, *Prog. Part. Nucl. Phys.* **4** (1980) 451.
5. P. J. Karol, *Phys. Rev.* **C33** (1975) 1203.
6. E. M. Friedlander, H. H. Heckman and Y. Karant, *Phys. Rev.* **C27** (1983) 2436.
7. I. S. Gradshteyn and I. M. Ryzhik, *Table of Integrals, Series and Products* (Academic Press Inc., 1965) Eq. (3.323.2).